ONCOLOGY

Multiparameter MRI-based radiomics for preoperative prediction of extramural venous invasion in rectal cancer

Zhenyu Shu[1] · Dewang Mao[1] · Qiaowei Song[1] · Yuyun Xu[1] · Peipei Pang[2] · Yang Zhang[1]

Abstract

Objectives To compare multiparameter MRI-based radiomics for preoperative prediction of extramural venous invasion (EMVI) in rectal cancer using different machine learning algorithms and to develop and validate the best diagnostic model.
Methods We retrospectively analyzed 317 patients with rectal cancer. Of these, 114 were EMVI positive and 203 were EMVI negative. Radiomics features were extracted from T_2-weighted imaging, T_1-weighted imaging, diffusion-weighted imaging, and enhanced T_1-weighted imaging of rectal cancer, followed by the dimension reduction of the features. Logistic regression, support vector machine, Bayes, K-nearest neighbor, and random forests algorithms were trained to obtain the radiomics signatures. The area under the receiver operating characteristic curve (AUC) was used to evaluate the performance of each radiomics signature. The best radiomics signature was selected and combined with clinical and radiological characteristics to construct a joint model for predicting EMVI. Finally, the predictive performance of the joint model was assessed.
Results The Bayes-based radiomics signature performed well in both the training set and the test set, with the AUCs of 0.744 and 0.738, sensitivities of 0.754 and 0.728, and specificities of 0.887 and 0.918, respectively. The joint model performed best in both the training set and the test set, with the AUCs of 0.839 and 0.835, sensitivities of 0.633 and 0.714, and specificities of 0.901 and 0.885, respectively.
Conclusions The joint model demonstrated the best diagnostic performance for the preoperative prediction of EMVI in patients with rectal cancer. Hence, it can be used as a key tool for clinical individualized EMVI prediction.

Key Points

• *Radiomics features from magnetic resonance imaging can be used to predict extramural venous invasion (EMVI) in rectal cancer.*
• *Machine learning can improve the accuracy of predicting EMVI in rectal cancer.*
• *Radiomics can serve as a noninvasive biomarker to monitor the status of EMVI.*

Keywords Rectal neoplasms · Multiparametric magnetic resonance imaging · Nomograms · Algorithms

Abbreviations

ACI	Anal canal invasion
ADC	Apparent diffusion coefficient
AIC	Akaike's information criterion
AUC	Area under the curve
CC	Correlation coefficient
CEA	Carcinoembryonic antigen
CRM	Circumferential resection margin
CT	Computed tomography
DIS	Distance from the end of the convex edge of the tumor to the edge of the anus
DWI	Diffusion-weighted imaging
EMVI	Extramural venous invasion
IMV	Inferior mesenteric vein
KNN	K-nearest neighbor
LR	Logistic regression
mpMRI	Multiparameter magnetic resonance imaging
mrEMVI	MpMRI-based extramural venous invasion

Zhenyu Shu and Dewang Mao contributed equally to this work.

✉ Yang Zhang
18701853713@163.com

1   Department of Radiology, Zhejiang Provincial People's Hospital, Affiliated People's Hospital, Hangzhou Medical College, Hangzhou, Zhejiang, China

2   Department of Pharmaceuticals Diagnosis, GE Healthcare, Hangzhou, China

PACS	Picture archiving and communication system
RF	Random forests
ROC	Receiver operating characteristic curve
RSD	Relative standard deviation
SRV	Superior rectal vein
SVM	Support vector machine
T_1WI	T_1-weighted imaging
T_2WI	T_2-weighted imaging
VOI	Volume of interest

Introduction

Colorectal cancer is the second leading cause of cancer-related deaths globally, with rectal cancer alone accounting for one-third of these cases [1]. Extramural venous invasion (EMVI) is defined as the presence of tumor cells in blood vessels located beyond the muscularis propria in the mesorectal fat. Interstitial adipose tissue around the tumor is at an increased risk of vascular invasion, which, in turn, significantly increases the risk of distant metastasis. Hence, EMVI can be considered a significant predictor of both the local recurrence and distant metastasis in rectal cancer [2, 3]. Therefore, EMVI is used for routine assessment and to identify risk stratification indicators in rectal cancer [4]. Accurate identification of the EMVI status is crucial for treatment decisions and prognosis.

Multiparameter magnetic resonance imaging (mpMRI) is the first choice for early noninvasive assessment of rectal cancer and detection of EMVI [5]. However, mpMRI has limited spatial resolution. It cannot be used to accurately diagnose the invasion of vessels smaller than 3 mm [6]. It is also sometimes difficult to distinguish such small blood vessels from small lymphatic vessels and peritoneal reverse folds [7]. In addition, inflammation, edema, and fibrosis may also adversely affect the mrEMVI evaluation [8]. Therefore, visual assessment based on mpMRI alone may not be sufficient to accurately identify EMVI. Hence, there is an urgent need to develop an objective, noninvasive, and accurate method for the preoperative evaluation of EMVI.

Radiomics uses big data mining techniques to analyze the correlation between radiological characteristics and pathological data. Hence, it is a powerful tool to provide decision support in oncology [9, 10]. Radiomics has been successfully used for the diagnosis, treatment, and prognosis of rectal cancer [11]. A recent study has also shown that radiomics is a superior tool to predict the occurrence of EMVI in rectal cancer [12]. However, such studies used only a single sequence. In contrast, mpMRI can often provide more useful information [13]. Additionally, predictive and prognostic models are important in radiomics [14]. Highly accurate and reliable models are needed in clinical practice to improve the decision-making process, which can be achieved through machine learning algorithms [15]. Accordingly, we hypothesize that more valuable radiomics features could be extracted using mpMRI and a new model can be constructed through machine learning for better prediction and stratification of the EMVI state.

The purpose of this study is to apply mpMRI-based radiomics to preoperatively predict the EMVI status of rectal cancer using different machine learning algorithms to build the best radiomics signature and to develop and validate the joint model by combining the radiomics signature and clinical and radiological characteristics.

Materials and methods

Patients

The study design was approved by our institutional ethics committee and the need for informed consent was waived off (No. 2021QT211). For this retrospective study, 1123 patients with rectal cancer confirmed between January 2017 and January 2021 were identified from a picture archiving and communication system (PACS). Among these patients, 317 were finally selected for the study based on the following inclusion criteria: (1) pathologically confirmed rectal cancer; (2) complete clinical and radiological data; (3) no history of other malignant tumors; and (4) no preoperative antitumor treatments. The exclusion criteria were as follows: (1) incomplete pathological data; and (2) poor imaging quality of mpMRI. In addition, the patients diagnosed between January 2017 and December 2019 were grouped into a training set ($n = 221$). This training set was used to test the robust features of radiomics and construct a model. Those diagnosed between January 2020 and January 2021 were grouped into a test set ($n = 96$) for validating the reliability of the model. A flowchart for patient recruitment is shown in Fig. 1.

Clinical and radiological data

The clinical and radiological data of all patients were retrospectively analyzed from our PACS, including data on age, gender, carcinoembryonic antigen (CEA) level, EMVI status, mpMRI-based radiological tumor (T) stage, lymph node (N) stage, tumor long diameter, transverse diameter, anteroposterior diameter, tumor volume, distance (DIS), circumferential resection margin (CRM), anal canal invasion (ACI), and mrEMVI status [16]. The postoperative pathological tissue was used as the reference standard for EMVI status. These features were independently assessed by two experienced radiologists. For the purpose of this study, the quantitative measurements obtained by the two radiologists were averaged for further analysis. For qualitative

Fig. 1 Flowchart for recruitment of patients in this study (Note. PACS, picture archiving and communication system; EMVI, extramural venous invasion; T stage, tumor stage)
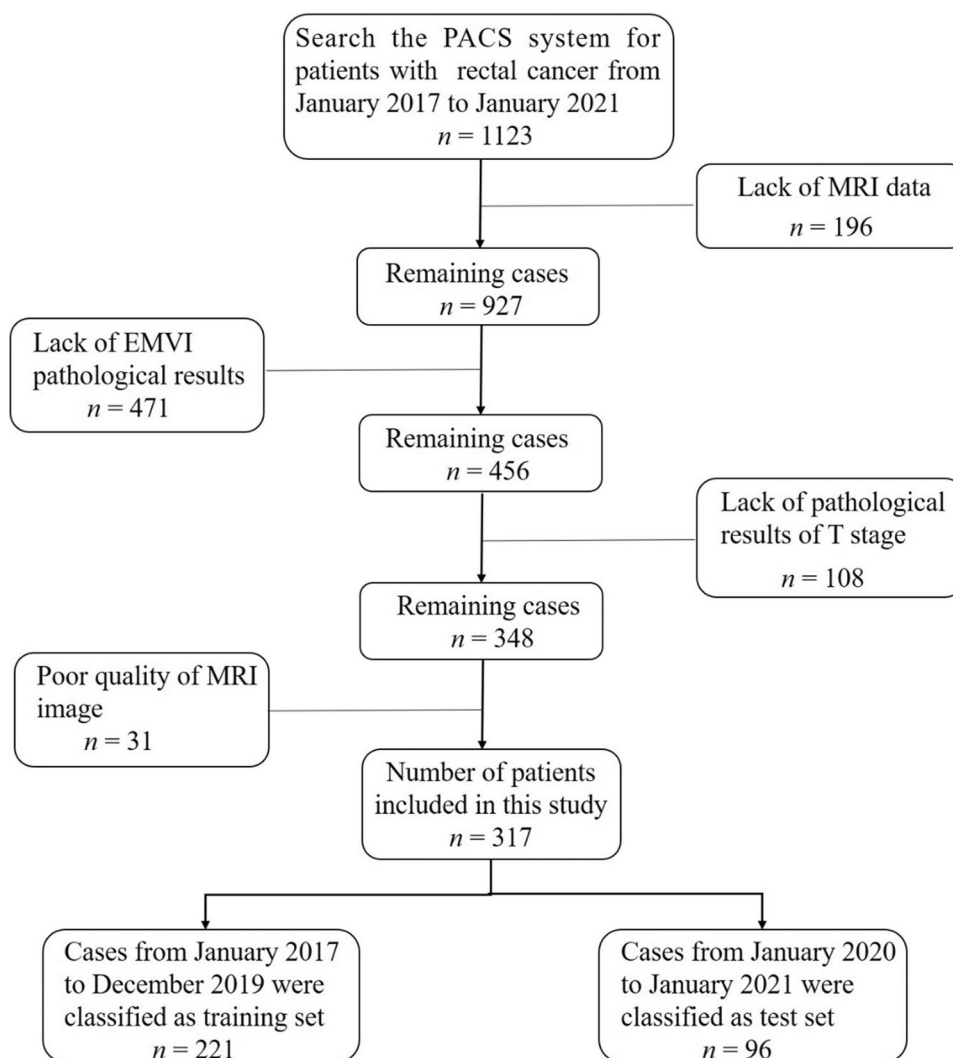
parameters, these two radiologists carefully reviewed all the images until a consensus was reached. Detailed information can be found in the Supplementary Materials.

Image preprocessing and segmentation

All patients underwent mpMRI examination, which was performed using a 3.0-T MRI scanner (Skyra; Siemens Healthineers). The image protocols and detailed parameters are provided in Supplementary Materials and Table S1. Noncommercial A.K. Software (Analysis Kit, GE Healthcare) was used for image preprocessing and registration of T_2-weighted imaging (T_2WI), T_1-weighted imaging (T_1WI), diffusion-weighted imaging (DWI), and enhanced T_1-weighted imaging (T_1+C) sequences before extracting the features in order to reduce the potential influence of the parameters of a scanning scheme. The T_2WI sequences on the axial plane were collected on an oblique-axial plane perpendicular to the rectum axis. Image preprocessing was performed by resampling the images with a resolution of $1 \times 1 \times 1$ mm^3 through the linear interpolation method and by discretizing and normalizing the image gray level to order 32. Then, the registration function of the A.K. Software was used to adopt T_2WI as the template for rigid registration of all sequences to ensure that the four sequences contained the same resolution, spacing, and origin. The standardized T_2WI images were imported into the ITK Software to segment the entire rectal tumor layer by layer to determine the volume of interest (VOI). Depending on the registration of different sequences, T_1WI, DWI, and T_1+C can share the same VOI obtained from T_2WI. Finally, the VOIs were imported into A.K. Software for feature extraction.

Extraction and selection of radiomics features

We extracted 378 radiomics features from each sequence, including 42 histogram features, 10 Haralick features, 9 form factor features, 126 Gray-level co-occurrence matrix
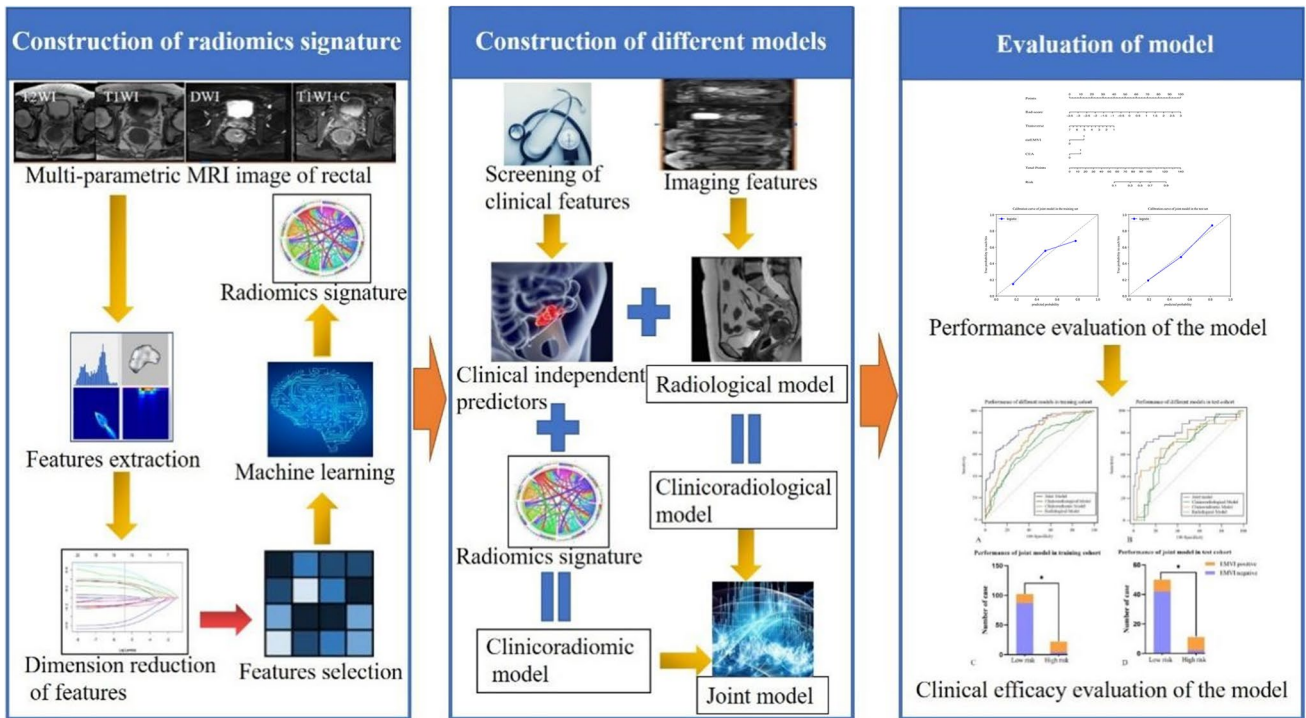
Fig. 2 Construction and evaluation of different models

Table 1 Clinical and radiological characteristics of patients in the training and test sets

Characteristics		Training set ($n=221$)	Test set ($n=96$)	p value
Age (years, SD)		64.08 (10.52)	63.78 (10.32)	0.814
Gender (male, %)		157 (71.04)	67 (69.79)	0.822
CEA (abnormal, %)		97 (43.89)	34 (35.42)	0.159
Long diameter (cm, SD)		3.79 (1.39)	3.89 (1.53)	0.586
Transverse diameter (cm, SD)		2.97 (1.18)	2.96 (1.17)	0.904
Anteroposterior diameter (cm, SD)		1.31 (0.65)	1.23 (0.67)	0.353
Tumor volume (cm^3, SD)		19.19 (23.43)	18.49 (28.03)	0.817
DIS (cm, SD)		8.04 (3.69)	8.11 (4.07)	0.880
CRM status (positive, %)		54 (24.43)	22 (22.92)	0.771
mrEMVI status (positive, %)		53 (23.98)	28 (29.17)	0.331
ACI status (positive, %)		13 (5.88)	4 (4.17)	0.533
Lymph node (metastasis, %)		139 (62.90)	62 (64.58)	0.774
Radiological tumor stage (N, %)	T_{1-2}	59 (26.70)	27 (28.12)	0.793
	T_{3-4}	162 (73.30)	69 (71.88)	

Note. *CEA*, carcinoembryonic antigen; *DIS*, distance from the end of the convex edge of the tumor to the edge of the anus; *CRM*, circumferential resection margin; *mrEMVI*, MRI-based extramural vascular invasion; *ACI*, anal canal invasion. Data are presented as counts or means (standard deviations in parentheses)

features, 180 run-length matrix features, and 11 Gray-level size zone matrix features. Four sequences were scanned in one patient, affording 1512 radiomics features per patient. In addition, tumor segmentation was manually delineated independently by two radiologists (radiologist A and radiologist B) using ITK software to ensure the stability and accuracy of the radiomics features, and feature set A (from radiologist A) and feature set B (from radiologist B) were obtained. Spearman's rank correlation test was used to calculate the correlation coefficient (CC) of each feature in sets A and B. Features with $CC > 0.8$ were considered robust.

Table 2 Characteristics of patients in the EMVI and non-EMVI groups in the training and test sets

Characteristics		Training set ($n=221$)			Test set ($n=96$)		
		Non-EMVI ($n=142$)	EMVI ($n=79$)	p value	Non-EMVI ($n=61$)	EMVI ($n=35$)	p value
Age (years, SD)		63.8 (10.7)	64.58 (10.23)	0.599	64.11 (8.6)	63.2 (12.89)	0.709
Gender (male, %)		102 (71.83)	55 (69.62)	0.729	44 (72.13)	23 (65.71)	0.512
CEA (abnormal, %)		52 (36.62)	45 (56.96)	0.003*	17 (27.88)	17 (48.57)	0.041*
Long diameter (cm, SD)		3.90 (1.42)	3.59 (1.32)	0.112	3.79 (1.49)	4.05 (1.61)	0.416
Transverse diameter (cm, SD)		3.09 (1.2)	2.77 (1.13)	0.056	2.95 (1.1)	2.96 (1.31)	0.972
Anteroposterior diameter (cm, SD)		1.35 (0.66)	1.23 (0.64)	0.215	1.25 (0.7)	1.21 (0.62)	0.779
Tumor volume (cm^3, SD)		21.13 (23.95)	15.72 (22.19)	0.100	18.59 (30.5)	18.31 (23.53)	0.962
DIS (cm, SD)		8.01 (3.4)	8.09 (4.17)	0.881	6.6 (4.4)	6.1 (2.3)	0.365
CRM status (positive, %)		31 (21.83)	23 (29.11)	0.227	7 (11.48)	15 (42.86)	<0.001*
mrEMVI status (positive, %)		25 (17.61)	28 (35.44)	0.003*	10 (16.39)	18 (51.43)	<0.001*
ACI status (positive, %)		8 (5.63)	5 (6.33)	0.930	1 (1.64)	3 (8.57)	0.269
Lymph node (metastasis, %)		83 (58.45)	56 (70.89)	0.067	34 (55.74)	28 (80)	0.017*
Radiological tumor stage (N, %)	T_{1-2}	46 (32.39)	13 (16.46)	0.010*	25 (40.98)	2 (5.71)	<0.001*
	T_{3-4}	96 (67.61)	66 (83.54)		36 (59.02)	33 (94.29)	

Note. *EMVI*, patients with pathologic extramural venous invasion; *Non-EMVI*, patients without pathologic extramural venous invasion; *CEA*, carcinoembryonic antigen; *DIS*, distance from the end of the convex edge of the tumor to the edge of the anus; *CRM*, circumferential resection margin; *mrEMVI*, MRI-based extramural vascular invasion; *ACI*, anal canal invasion. Data are presented as counts or means (standard deviations in parentheses)

Construction and validation of radiomics signatures

Dimension reduction of the robust features selected was performed using the training set. More information can be found in the Supplementary Materials. On the basis of the retained features, we selected five machine learning algorithms—logistic regression (LR), support vector machine (SVM), Bayes, k-nearest neighbor (KNN), and random forests (RF)—to construct radiomics signatures. To select the best machine learning algorithm, we used the relative standard deviation (RSD) and Bootstrap method to quantify the stability of the five algorithms. The machine learning algorithm with the minimum RSD value was selected as the best algorithm to construct the radiomics signature. Detailed information about the RSD can be found in the Supplementary Materials. Finally, to quantify the signature discriminability, a machine learning score of each patient was calculated using the radiomics signature model. This result reflected the possibility of EMVI and was defined as the RAD score.
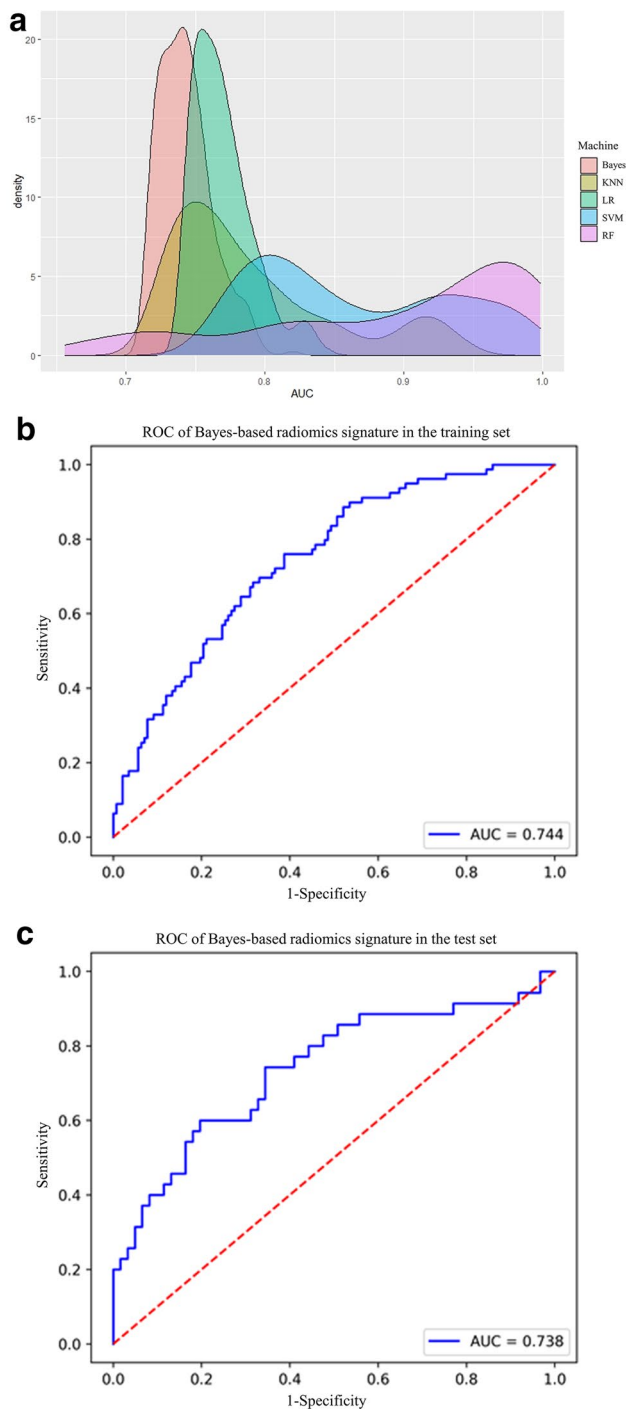
Model construction and evaluation

Multivariate logistic regression analysis and backward stepwise selection method with the stopping rule based on Akaike's information criterion (AIC) were conducted to select independent predictors from clinical and radiological variables, based on which a joint model was built. To verify the improvement in the performance of the model after including the radiomics signature, we used the selected independent predictors to construct different combined models. We used the area under the receiver operating characteristic (ROC) curves (AUC) to evaluate the performance of different models. In addition, we used the DeLong test to determine the difference between the joint model and other combined models. To assess the clinical efficacy of the joint model, we developed a visual nomogram to calculate the probability of EMVI for each patient. Finally, we used the Hosmer–Lemeshow test to analyze the goodness-of-fit of the nomogram and employed the calibration curve to visually assess the consistency between the predicted and actual EMVI probabilities. We used the optimal cut-off value corresponding to the Youden index of the ROC curve as the threshold. Using the EMVI probability of each patient, we grouped patients with negative mrEMVI into high-risk and low-risk groups and compared their pathological EMVI results. The construction and evaluation of different models are shown in Fig. 2.

Statistical analysis

Statistical analyses were performed with SPSS software (version 24.0), MedCalc software (version 11.2), and Python (version 3.5). The continuous variables were compared by performing a two-sample t-test or the Mann–Whitney *U* test,

a

b

ROC of Bayes-based radiomics signature in the training set

c

ROC of Bayes-based radiomics signature in the test set

Fig. 3 Density distribution of the area under the receiver operating characteristic (AUC) curve of radiomics signatures constructed by five machine learning algorithms (**a**) and diagnostic efficiency of the Bayes-based radiomics signature for predicting extramural venous invasion in the training set (**b**) and the test set (**c**)

and the categorical variables were compared by a chi-square test. The ROC curves were used to evaluate the predictive performance of different models. The metrics included AUC,

sensitivity, and specificity. All statistics were two-way, and the statistical significance was set at $p < 0.05$.

Results

Characteristics of the patients

No statistical differences were noted between the clinical and radiological characteristics of the training and test sets ($p = 0.159$–0.904), as shown in Table 1. In contrast, statistical differences were observed in CEA, mrEMVI, and tumor stage of both the EMVI and non-EMVI groups in the training and test sets ($p < 0.05$). In addition, we observed statistical differences between the EMVI and non-EMVI groups in terms of the lymph node ($p = 0.017$) and CRM ($p < 0.001$) status in the test set. The characteristics of the patients in the EMVI and non-EMVI groups in the training and test sets are detailed in Table 2.

Performance of radiomics signatures

Of the 1512 radiomics features in the training set, we selected 793 as robust features and used them for dimension reduction. Finally, 20 features were retained from the four sequences— T_2WI ($n = 4$), T_1WI ($n = 6$), DWI ($n = 7$), and $T_1 + C$ ($n = 3$)— to construct the radiomics signatures. These features have been detailed in the Supplementary Materials. The RSD values of the radiomics signatures based on LR, SVM, Bayes, KNN, and RF were 2.72, 8.13, 2.43, 7.46, and 11.01, respectively. Therefore, Bayes was chosen as the machine learning algorithm for constructing the radiomics signature in this study. The Bayes-based radiomics signature performed well in both the training and test sets, with the AUCs of 0.744 and 0.738, sensitivities of 0.754 and 0.728, and specificities of 0.887 and 0.918, respectively, as shown in Fig. 3.

Model construction and comparison

CEA ($p = 0.043$), mrEMVI ($p = 0.039$), transverse diameter ($p = 0.003$), and radiomics signature ($p < 0.001$) were determined using multivariate logistic regression analysis and selected as independent predictors (Table 3) to construct the joint model and develop the visual nomogram (Fig. 4a). Calibration curves of the joint model for predicting the EMVI demonstrated good agreement with the ideal curve in both the training set (Fig. 4b) and the test set (Fig. 4c). The Hosmer–Lemeshow test yielded no significant difference between the predictive calibration curve and the ideal curve for EMVI prediction in the training set ($p = 0.745$). In addition, the joint model performed better than MRI in predicting the EMVI, as shown in Fig. 5.

Table 3 Results of univariate and multivariate logistic regression analyses

Variables	Univariate logistic regression		Multivariate logistic regression	
	OR(95%CI)	*p* value	OR(95%CI)	*p* value
Age	1.007 (0.981,1.034)	0.597	NA	NA
Gender	1.113 (0.609, 2.034)	0.728	NA	NA
CEA	2.291 (1.307, 4.015)	0.004*	1.868 (0.997, 3.500)	0.043*
Long diameter	0.846 (0.687, 1.041)	0.114	NA	NA
Transverse diameter	0.788 (0.615, 1.008)	0.007*	0.64 (0.476,0.859)	0.003*
Anteroposterior diameter	0.752 (0.479, 1.181)	0.216	NA	NA
Tumor volume	0.988 (0.974, 1.003)	0.110	NA	NA
DIS	1.006 (0.934, 1.084)	0.873	NA	NA
CRM status	1.471 (0.785, 2.755)	0.229	NA	NA
mrEMVI status	2.569 (1.366, 4.832)	0.003*	2.071 (1.038, 4.131)	0.039*
ACI status	1.132 (0.357, 3.585)	0.833	NA	NA
Lymph node	1.731 (0.960, 3.119)	0.068	NA	NA
Radiological tumor stage	2.433 (1.219, 4.854)	0.012*	NA	NA
Radiomics signature	2.718 (1.892, 3.905)	<0.001*	2.611 (1.815, 3.757)	<0.001*

Note. *CEA*, carcinoembryonic antigen; *DIS*, distance from the end of the convex edge of the tumor to the edge of the anus; *CRM*, circumferential resection margin; *mrEMVI*, MRI-based extramural vascular invasion; *ACI*, anal canal invasion; *OR*, odds ratio

The radiological model was constructed using mrEMVI and transverse diameter; the clinicoradiological model was constructed using CEA, mrEMVI, and transverse diameter; and the clinicoradiomic model was constructed using CEA and radiomics signature. Among the four different models, the joint model performed best with the AUCs of 0.839 and 0.835, sensitivities of 0.633 and 0.714, and specificities of 0.901 and 0.885 in the training and test sets, respectively. The DeLong test showed that the joint model was statistically different from the other three combined models in both the training and test sets ($p < 0.05$), highlighting the improved predictive performance of the radiomics signature, as shown in Table 4 and Fig. 6a, b.

The optimal threshold of 0.5545 was selected in the ROC analysis based on the Youden Index of the joint model for patients with negative mrEMVI. Patients with model scores of > 0.5545 were predicted as high-risk cases, while those with scores of < 0.5545 were predicted as low-risk cases. The number of patients with a positive pathological EMVI status in the low-risk and high-risk groups in both the training and test sets was significantly different, indicating the clinical applicability of the nomogram, as shown in Fig. 6c, d.

Discussion

We compared mpMRI-based radiomics for preoperatively predicting the EMVI status of rectal cancer using five machine learning algorithms and observed that the Bayes-based radiomics signature performed well. Our results showed that radiomics can be used for predictions, which further validated Zech et al.'s proposal that the EMVI can be used as a new imaging biomarker for the prognosis of rectal cancer [3]. In addition, the joint model showed significantly improved prediction performance for EMVI. The nomogram can also provide good classification and recognition for patients with the negative mrEMVI status, which may be used as a convenient and accurate tool to identify and predict the EMVI.

The mrEMVI assessment mainly depended on the scanning technique and subjective imaging analysis [17]. However, radiologists often find it difficult to use, which may lead to misdiagnosed prediction of EMVI [18]. Our study also confirmed this phenomenon. The radiological model based on mrEMVI showed poor performance in the preoperative prediction of EMVI. In contrast, the joint model demonstrated the best diagnostic performance in both the training set (AUC = 0.839) and the test set (AUC = 0.835). Encouragingly, the joint model can also afford good classification and recognition in patients with negative mrEMVI, further demonstrating its superiority, which may also be due to its high specificities (90.1% and 88.5% in the training and test sets, respectively). Of course, the joint model showed such a superior performance because of the inclusion of the radiomics signature. In fact, the radiomics signature itself outperformed the radiological model in the test set (AUC: 0.738 vs 0.647). The application of machine learning algorithm and multiparameter radiomics features was the main reason for the better diagnostic performance of the radiomics signature.
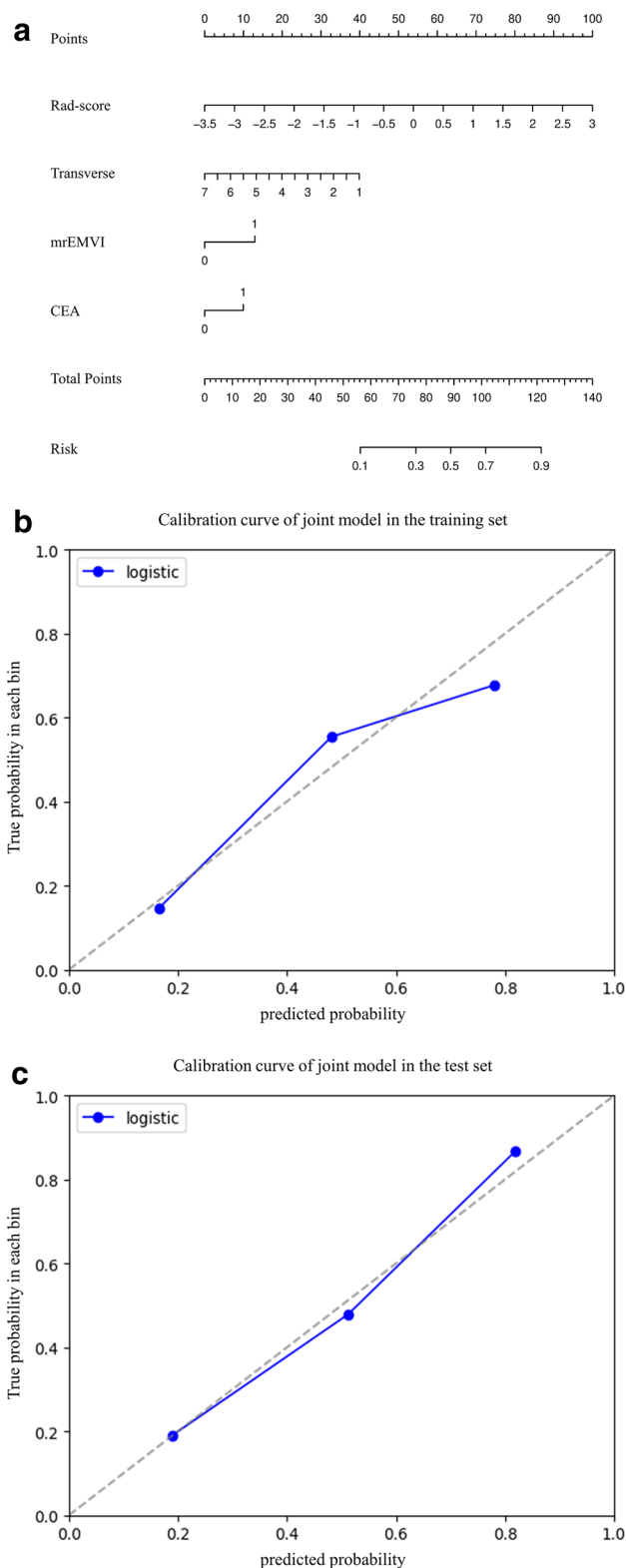
Fig. 4 Visual nomogram based on the joint model (**a**). Calibration curves of the joint model for predicting extramural venous invasion in the training set (**b**) and the test set (**c**), which demonstrated good agreement with the ideal curve (Note. mrEMVI, MRI-based extramural vascular invasion; CEA, carcinoembryonic antigen)

Machine learning algorithms have been widely applied in the field of radiomics, which greatly improve diagnostic performance [19]. The LR is currently the most widely used machine learning algorithm because of its simplicity. Although the diagnostic efficiency of the LR is higher than that of the Bayes, the latter was more stable than the former in our study. The stability of the radiomics model is also highly important for its clinical application. Therefore, we chose the Bayes to construct the radiomics signature. In addition, multiparameter features may contain more information, which allows for a more comprehensive characterization of the tumor [20]. The sensitivity and specificity of the radiomics signature for EMVI prediction as observed in our study are significantly higher than those reported by Roberto et al. using DWI and T_2WI [21], which further demonstrated the great potential of the multiparameter radiomics features.

Previous studies have identified the tumor size, location, T staging, and N staging as the risk factors for EMVI [22, 23]. In contrast, our study showed that only the transverse diameter, which is related to the tumor size, can be used as an independent predictor of EMVI. This result indirectly showed that the transverse diameter may help in determining the impact of tumor size on prognosis, further validating the findings of Yoshimoto et al. that the tumor diameter can be used as a prognostic indicator of colorectal cancer [24]. Our study also showed that CEA is an independent predictor of EMVI. CEA, a large glycoprotein, has been proposed as a prognostic biomarker that can be used to determine the prognosis and stage of colorectal cancer [25, 26]. Although mrEMVI is still the most favorable independent predictor, it is important to note that the radiological model based on mrEMVI and transverse diameter performed poorly in predicting EMVI, perhaps owing to the inherent defects of the visual subjective imaging analysis. Despite this drawback, it cannot be denied that mrEMVI is still one of the important contents routinely used in mpMRI-based imaging analysis [27].

A previous study [28] has reported that the computed tomography (CT)–based superior hemorrhoidal vein diameter had a better discrimination power in predicting the EMVI (AUC = 0.83, sensitivity = 88.2%, specificity = 94.6%) than our joint model. However, our model may be more suitable for clinical practice than CT, because the latter causes radiation damage. Aysegul et al. used changes in the diameters of the superior rectal vein (SRV) and inferior mesenteric vein (IMV), and apparent diffusion coefficient (ADC) values for EMVI prediction [29]; their AUC values were 0.851, 0.893, and 0.664, respectively. Although the AUCs of CT-based SRV and IMV were higher than those of our joint model, the AUC of the MRI-based ADC value was significantly lower than that of our model. In addition, the specificities of our joint model (90.1% and 88.5% in the training and test sets,
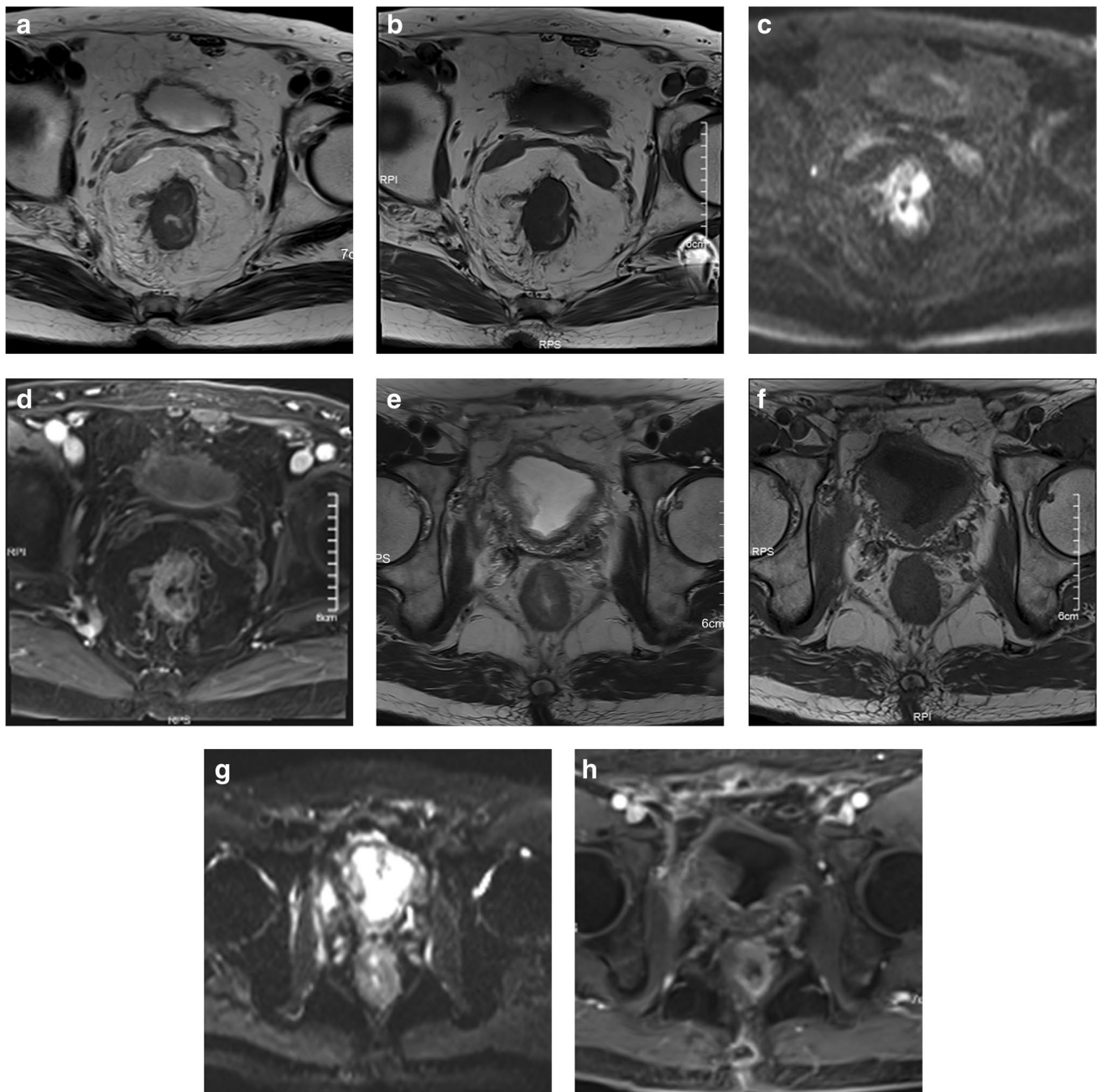
Fig. 5 Two cases with rectal cancer and positive extramural venous invasion (EMVI) at histopathologic examination. **a–d** One case had obvious EMVI on MRI, which could also be detected by the joint model. **e–h** The other was EMVI detected by the joint model, which was not apparent on MRI

respectively) are significantly higher than those reported by Aysegul et al. (67.9%, 71.4%, and 57.1% for SRV, IMV, and ADC, respectively). A previous study showed that functional imaging such as DWI cannot improve the efficiency of EMVI detection [30]. Yu et al. combined DCE and clinical-pathological factors to construct a radiomics model to predict EMVI with an AUC of 0.904, sensitivity of 90.5%, and specificity of 79.2% [12]. Although this result

was significantly higher than that reported in the present study, it should be noted that the AUC was only 0.812 in the test set, indicating the poor stability of the model used by Yu et al. The AUC of our joint model reached 0.835 in the test set, probably because of its higher stability. In fact, the radiomics signature showed greater variability than the clinical characteristics [31]. We used a stable machine learning algorithm and multiparameter radiomics features to

Table 4 Predictive performance of different models in the training and test sets

Models	Training set			Test set		
	AUC (95%CI)	Sensitivity	Specificity	AUC (95%CI)	Sensitivity	Specificity
Joint model	0.839 (0.784–0.885)	0.633	0.901	0.835 (0.745–0.903)	0.714	0.885
Clinicoradiological model	0.683 (0.617–0.744)	0.772	0.514	0.675 (0.572–0.767)	0.713	0.639
Clinicoradiomic model	0.761 (0.699–0.816)	0.873	0.528	0.726 (0.626–0.813)	0.657	0.754
Radiological model	0.649 (0.582–0.712)	0.506	0.732	0.647 (0.543–0.742)	0.571	0.732

Note. *AUC*, area under the receiver operating characteristic curve
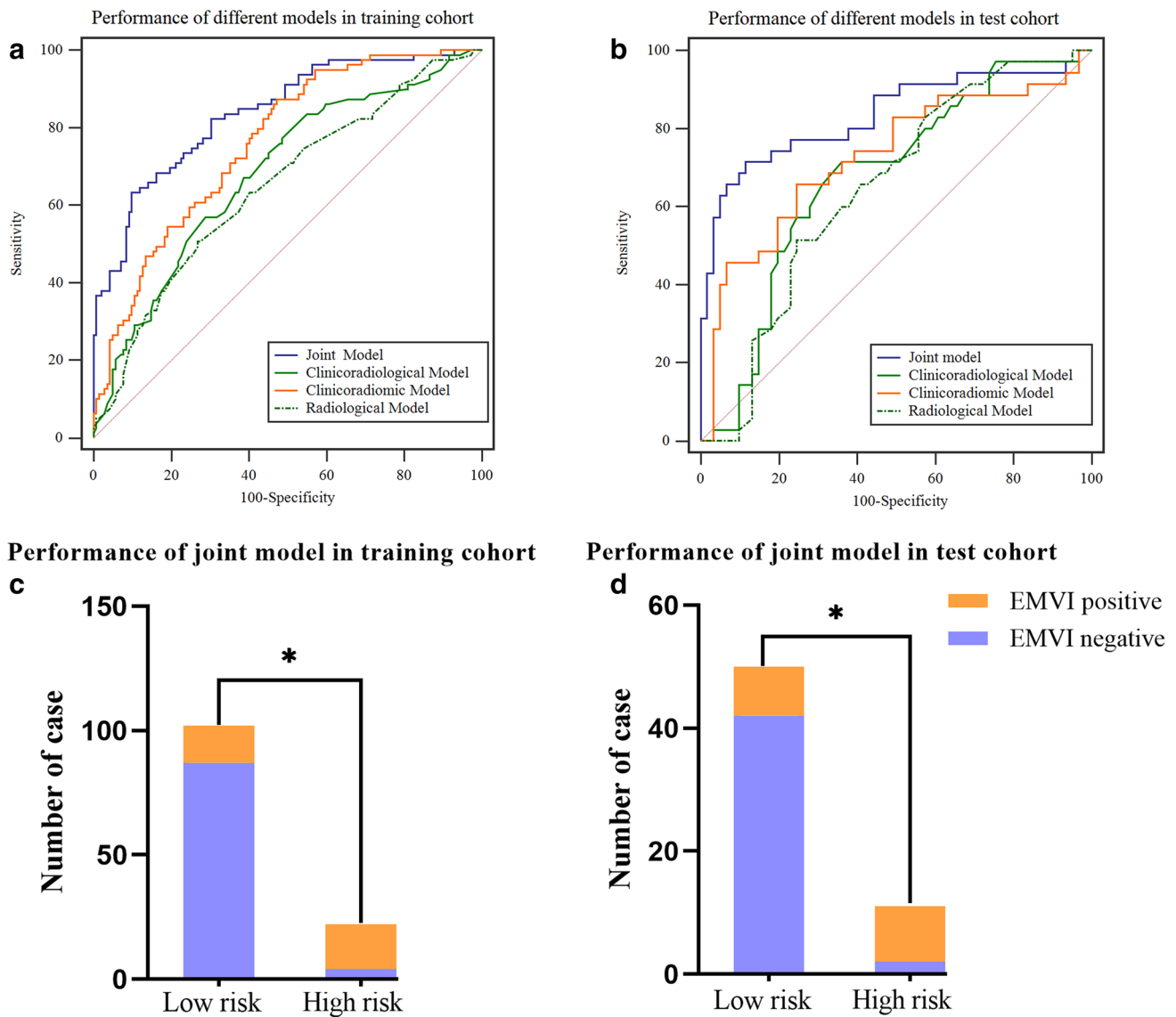
Fig. 6 Diagnostic performance for extramural venous invasion prediction of different models in the training (**a**) and test (**b**) sets. Negative mrEMVI patients were divided into high-risk and low-risk cases according to the nomogram. The probability of pathological EMVI in the high-risk group was significantly higher than that in the low-risk group in both the training (**C**) and test (**D**) sets. (Note. * means $p < .05$; EMVI, extramural venous invasion; mrEMVI, MRI-based extramural vascular invasion)

overcome the variability in the radiomics signature of our study, which may provide a new idea for conducting future radiomics research in clinical practice.

In addition, our joint model has good clinical applicability, because the model construction is mainly based on noninvasive mpMRI examination and image analysis. The measurement of another construction feature, CEA, depends on the routine test item for each hospitalized patient. As the test cost is low, it is suitable for clinical development. We also built a nomogram based on the joint model, which enables clinicians to more conveniently and quickly quantifies the EMVI status of patients. Therefore, our study provides a reliable, convenient, and rapid tool to predict the EMVI status in clinical practice.

Our research has some limitations as well. Firstly, it is a retrospective study. However, the eligible patients were consecutively retrieved from a prospective database that included all patients with rectal cancer in our hospital. Secondly, the pathological evaluation could not be checked for consistency because of the retrospective design. Nevertheless, the pathologic EMVI status used for training the radiologist was basically reliable, although it was difficult to ensure that the pathologic EMVI status was correct for every patient. Thirdly, this research lacks external validation because of data confidentiality, which we aim to resolve in our future work. Finally, there is a discrepancy between the number of EMVI-positive and EMVI-negative patients. However, it did not have any effect on our results, because the proportion of EMVI-positive and EMVI-negative patients is approximately the same in both groups.

Conclusion

This study showed that mpMRI-based radiomics can improve the diagnostic performance of preoperative EMVI prediction in patients with rectal cancer, especially for inexperienced radiologists and residents. The visual nomogram based on the radiomics signature is a useful tool to avoid misdiagnosis to a great extent caused by the inexperience of radiologists. The study results also provided important evidence for the potential use of the joint model for risk stratification of rectal cancer in the future.

Declarations

References

1. Siegel RL, Miller KD, Jemal A (2018) Cancer statistics, 2018. CA Cancer J Clin 68:7–30
2. Chand M, Palmer T, Blomqvist L, Nagtegaal I, West N, Brown G (2015) Evidence for radiological and histopathological prognostic importance of detecting extramural venous invasion in rectal cancer: recommendations for radiology and histopathology reporting. Colorectal Dis 17:468–473
3. Zech CJ (2018) MRI of extramural venous invasion in rectal cancer: a new marker for patient prognosis? Radiology 289:686–687
4. Tudyka V, Blomqvist L, Beets-Tan RG et al (2014) EURECCA consensus conference highlights about colon & rectal cancer multidisciplinary management: the radiology experts review. Eur J Surg Oncol 40:469–475
5. Horvat N, Carlos Tavares Rocha C, Clemente Oliveira B, Petkovska I, Gollub MJ (2019) MRI of rectal cancer: tumor staging, imaging techniques, and management. Radiographics 39:367–387
6. Brown G, Radcliffe AG, Newcombe RG, Dallimore NS, Bourne MW, Williams GT (2003) Preoperative assessment of prognostic factors in rectal cancer using high-resolution magnetic resonance imaging. Br J Surg 90:355–364
7. Kim JY, Kim SH, Kim YJ et al (2015) Enhancement parameters on dynamic contrast enhanced breast MRI: do they correlate with prognostic factors and subtypes of breast cancers? Magn Reson Imaging 33:72–80
8. Bae JS, Kim SH, Hur BY et al (2019) Prognostic value of MRI in assessing extramural venous invasion in rectal cancer: multi-readers' diagnostic performance. Eur Radiol 29:4379–4388
9. Yip SS, Aerts HJ (2016) Applications and limitations of radiomics. Phys Med Biol 61:R150-166
10. Lambin P, Leijenaar RTH, Deist TM et al (2017) Radiomics: the bridge between medical imaging and personalized medicine. Nat Rev Clin Oncol 14:749–762
11. Horvat N, Bates DDB, Petkovska I (2019) Novel imaging techniques of rectal cancer: what do radiomics and radiogenomics have to offer? A literature review. Abdom Radiol (NY) 44:3764–3774
12. Yu X, Song W, Guo D et al (2020) Preoperative prediction of extramural venous invasion in rectal cancer: comparison of the diagnostic efficacy of radiomics models and quantitative dynamic contrast-enhanced magnetic resonance imaging. Front Oncol 10:459
13. Pham TT, Liney G, Wong K et al (2017) Study protocol: multiparametric magnetic resonance imaging for therapeutic response prediction in rectal cancer. BMC Cancer 17:465

14. Kumar V, Gu Y, Basu S et al (2012) Radiomics: the process and the challenges. Magn Reson Imaging 30:1234–1248
15. Yogesh S, Bhatia PK, Omprakash S (2007) A review of studies on machine learning techniques. Int J Comp Sci Security 1:70–84
16. Nougaret S, Reinhold C, Mikhael HW, Rouanet P, Bibeau F, Brown G (2013) The use of MR imaging in treatment planning for patients with rectal carcinoma: have you checked the "DIS-TANCE"? Radiology 268:330–344
17. Tripathi P, Rao SX, Zeng MS (2017) Clinical value of MRI-detected extramural venous invasion in rectal cancer. J Dig Dis 18:2–12
18. Smith NJ, Barbachano Y, Norman AR, Swift RI, Abulafi AM, Brown G (2008) Prognostic significance of magnetic resonance imaging-detected extramural vascular invasion in rectal cancer. Br J Surg 95:229–236
19. Giger ML (2018) Machine Learning in Medical Imaging. J Am Coll Radiol 15:512–520
20. Wei L, Osman S, Hatt M, El Naqa I (2019) Machine learning for radiomics-based multimodality and multiparametric modeling. Q J Nucl Med Mol Imaging 63:323–338
21. Fornell-Perez R, Vivas-Escalona V, Aranda-Sanchez J et al (2020) Primary and post-chemoradiotherapy MRI detection of extramural venous invasion in rectal cancer: the role of diffusion-weighted imaging. Radiol Med 125:522–530
22. Chen Y, Yang X, Wen Z et al (2019) Association between high-resolution MRI-detected extramural vascular invasion and tumour microcirculation estimated by dynamic contrast-enhanced MRI in rectal cancer: preliminary results. BMC Cancer 19:498
23. McClelland D, Murray GI (2015) A Comprehensive Study of Extramural Venous Invasion in Colorectal Cancer. Plos One 10:e0144987
24. Yoshimoto T, Morine Y, Imura S et al (2017) Maximum diameter and number of tumors as a new prognostic indicator of colorectal liver metastases. In Vivo 31:419–423
25. Duffy MJ, Lamerz R, Haglund C et al (2014) Tumor markers in colorectal cancer, gastric cancer and gastrointestinal stromal cancers: European group on tumor markers 2014 guidelines update. Int J Cancer 134:2513–2522
26. Locker GY, Hamilton S, Harris J et al (2006) ASCO 2006 update of recommendations for the use of tumor markers in gastrointestinal cancer. J Clin Oncol 24:5313–5327
27. Tripathi P, Guo W, Rao S, Zeng M, Hu D (2020) Additional value of MRI-detected EMVI scoring system in rectal cancer: applicability in predicting synchronous metastasis. Tumori 106:286–294
28. Wu CC, Lee RC, Chang CY (2013) Prediction of lymphovascular invasion in rectal cancer by preoperative CT. AJR Am J Roentgenol 201:985–992
29. GursoyCoruh A, Peker E, Elhan A, Erden I, Erden A (2019) Evaluation of extramural venous invasion by diffusion-weighted magnetic resonance imaging and computed tomography in rectal adenocarcinoma. Can Assoc Radiol J 70:457–465
30. Ahn JH, Kim SH, Son JH, Jo SJ (2019) Added value of diffusion-weighted imaging for evaluation of extramural venous invasion in patients with primary rectal cancer. Br J Radiol 92:20180821
31. Mayerhoefer ME, Materka A, Langs G et al (2020) Introduction to radiomics. J Nucl Med 61:488–495